VALIDATION OF SPECTRAL IMAGING DATABASE GENERATION FOR SKIN DIAGNOSIS THROUGH MONTE CARLO SIMULATION - REAL MEASUREMENT COMPARISON

Xuan Dat Ho[1], Nguyet Ha T. Tran[1], Thang V. Hoang[2], Tuan V. Pham[1], Anh Thu T. Nguyen[2]*

[1]LYDINC Institute of Education and Engineering - Technology, L.Y.D.I.N.C Co. Ltd., Da Nang, Vietnam
[2]The University of Danang - University of Science and Technology, Vietnam

*Corresponding address: ntathu@dut.udn.vn

(Received: May 15, 2025; Revised: June 18, 2025; Accepted: June 23, 2025)

DOI: 10.31130/ud-jst.2025.23(10B).650E

Abstract - Spectral imaging has recently gained attention as a promising noninvasive technique for diagnosing human skin conditions, owing to its safety and noninvasive nature. However, one of the main challenges to advancing the application of this technique is the lack of a comprehensive and reliable database capturing the optical characteristics of different skin tones and conditions. Monte Carlo Simulation on Multi-layer Media (MCML) has proven effective in modeling light-tissue interactions and generating spectral reflectance data for biological tissues, particularly skin. However, the traditional simulation process is time-consuming. This study examines and validates the results of an accelerated MCML simulation using CUDA technology, by comparing its spectral diffuse reflectance outputs with actual measurements from healthy skin across three distinct skin tones within the 900 nm to 1700 nm wavelength range. The high degree of agreement between simulated and measured data supports the feasibility of building a robust MCML-based spectral reflectance database.

Key words - MCML; skin health diagnosis; spectral imaging; AI; non-invasive techniques

1. Introduction

As demand for better dermatological care grows, the need for improved diagnostic services is increasingly evident worldwide and in Vietnam. In 2016, the American Academy of Dermatology (AAD) reported that 84.5 million Americans were affected by skin diseases, leading to $75 billion in healthcare costs [1]. Skin and subcutaneous disorders ranked as the fourth leading cause of nonfatal health issues globally in 2010 and 2013 [2]. In Vietnam, a survey by Binh Thuan Provincial Dermatology Hospital found that 41% of 2,400 respondents had atopic dermatitis, and 20.6% had fungal or parasitic skin conditions, largely due to air pollution and climate change [3]. In Ho Chi Minh City, the Dermatology Hospital treated an average of 120 pediatric patients daily for conditions like atopic dermatitis, allergic contact dermatitis, and fungal infections [4].

Despite advancements, current skin diagnostic methods remain inadequate for personal or widespread clinical use. Noninvasive optical imaging techniques, especially those enhanced by AI, are gaining traction in dermatology but are limited by the lack of a comprehensive skin database. Developing fast, accurate methods to expand this database is essential for improving accessible and efficient skin diagnostic solutions.

2. Methodology

2.1. Human skin structure

Human skin is a complex, multilayered organ with a highly individualized structure and chemical composition, which varies between individuals [5]. Diseases and conditions can visibly affect its structure and appearance [6]. Skin spectroscopy is a valuable technique for analyzing these changes by assessing the skin's optical properties and interaction with electromagnetic radiation. Specific wavelengths can reveal skin composition, abnormalities, or alterations through spectral measurements like absorbance and reflectance [7–8]. Spectroscopic analysis focuses on how light is reflected, absorbed, and transmitted through the skin layers [9], using specialized instruments to collect data across selected spectral ranges. Electromagnetic radiation is categorized by wavelength into radio waves, infrared (IR), visible light (VIS), ultraviolet (UV), X-rays, and gamma rays [10]. The depth of penetration and biological impact depend on energy and wavelength, with high-energy radiation (e.g., X-rays, gamma rays, certain UV rays) penetrating and damaging tissues. For most diagnostic applications, VIS and IR regions are preferred [10]. This study focuses on skin-light interaction in the 400 nm to 1700 nm range, which is safe for human tissue and provides sufficient information for modeling skin properties.

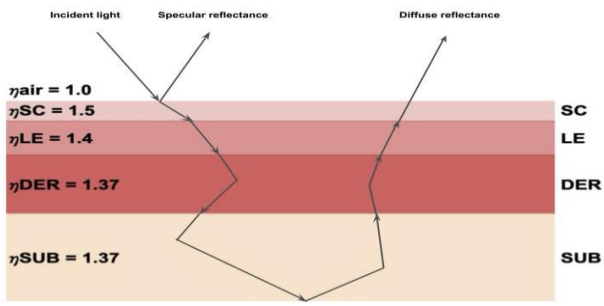

Figure 1. *General model of interaction between human skin and radiation [10]*

Human skin consists of three primary layers: the epidermis, dermis, and subcutis, each with sub-layers. Figure 1 illustrates radiation interaction with the skin. At the air-skin interface, part of the incoming light is reflected due to refractive index differences, while the rest is refracted into deeper layers. Each skin layer is

characterized by optical properties, including absorption coefficient (μa), scattering coefficient (μs), thickness (d), refractive index (η), and anisotropy factor (g).

In human skin, the outermost layer, the epidermis, consists of two sub-layers: the stratum corneum and the living epidermis. The stratum corneum, made up mainly of dead cells, acts as a protective barrier that retains moisture and prevents dehydration. It absorbs minimal light, with reflected light primarily considered surface reflectance. Below it, the living epidermis is composed of viable cells, with its optical properties mainly influenced by the pigment melanin [11, 12]. The dermis, beneath the epidermis, contains dense connective tissue with nerves and blood vessels. Hemoglobin, the natural chromophore in blood, absorbs light and gives the skin a reddish hue. There are two forms of hemoglobin: oxygenated (HbO_2) and deoxygenated (Hb) [13, 14]. Light scattering in this layer is mainly due to its fibrous structure. The innermost subcutis (or hypodermis), whose thickness varies by body region [15], has optical properties mainly influenced by water, fat cells, and hemoglobin.

2.2. Monte Carlo simulation

In Monte Carlo simulations, light is modeled as photons, ignoring wave-like properties such as phase change and polarization. Each photon is directed at the air-skin interface, where it interacts with skin tissues, scattering through layers until it is absorbed or exits as diffuse reflection. Photon propagation is governed by probability distributions, controlling step size and scattering angles. This study focuses on light interactions with wavelengths from 900 nm to 1700 nm, with details on Monte Carlo simulation for light-skin interactions at a specific wavelength, λ.

To simulate light-skin interaction at wavelength λ, parameters for each skin layer are required: absorption coefficient μa (cm^{-1}), scattering coefficient μs (cm^{-1}), thickness d (cm), anisotropy factor g (dimensionless), and refractive index η (dimensionless). For surrounding media, only refractive indices (η) are needed, set to 1 for air in this study, though other media like glass can be used. A grid of detectors measures photon absorption, fluence, reflectance, and transmittance, logging photon deposition in each grid element to calculate these quantities.

Initially, the Monte Carlo simulation is configured with three coordinate systems, as depicted in Figure 2, which outlines the flowchart for simulating multi-layered tissue. Each photon packet starts with an initial weight, W, set to one, along with a defined position and propagation direction. The photon's position is described by Cartesian coordinates (x, y, z), and its current direction of travel is represented by a unit vector, r. The corresponding directional cosines are:

$$\mu_x = \mathbf{r} \bullet \mathbf{x}$$
$$\mu_y = \mathbf{r} \bullet \mathbf{y} \qquad (2.2.1)$$
$$\mu_z = \mathbf{r} \bullet \mathbf{z}$$

where x, y, and z represent the unit vectors corresponding to these axes. The photon packet commences its journey at a predetermined angle. Upon reaching the interface between the air and the stratum corneum, which is the outermost layer of the skin in this model, the Fresnel effect takes place. This phenomenon results in a part of the photon packet being reflected away from the surface, while the remaining portion is refracted, or bent, and continues to transmit deeper into the skin tissue.

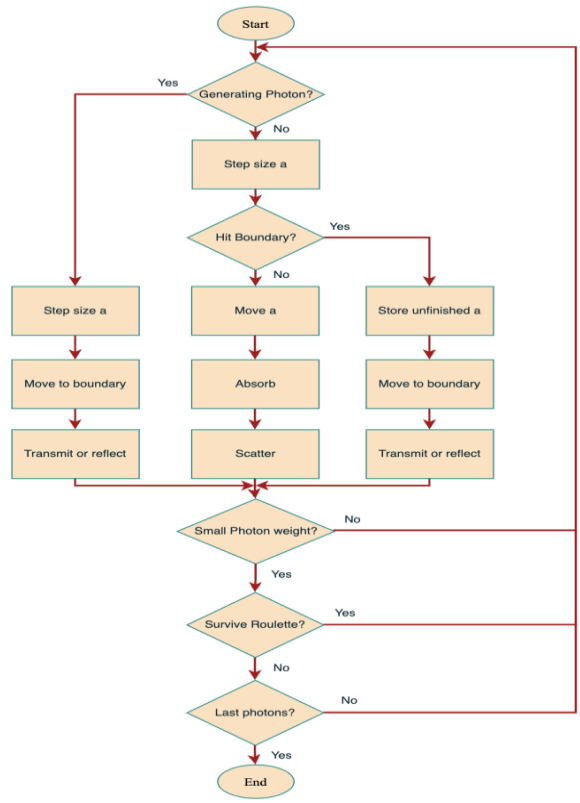

Figure 2. *Flowchart for Monte Carlo simulations [16]*

2.3. Modified CUDAMCML simulation program

The primary advantage of the Monte Carlo simulation method is its flexibility in modeling complex systems that are difficult to represent deterministically. However, it is computationally demanding due to the need to calculate probabilities for many photons. Due to CPU processing limitations, the simulation time was insufficient for database generation. To improve speed, the GPU-accelerated CUDAMCML program utilizes the computational power and parallel processing capabilities of GPUs. In this study, CUDAMCML was modified to address the limitation of normal incident light in original MCML-based simulations by calculating specular reflection using Fresnel's equations.

In CUDAMCML, photon packets are launched, and their steps are computed simultaneously across multiple threads. To maximize GPU parallelism, a new photon is launched immediately after the preceding one terminates. The program was updated to handle various incident angles and modern hardware. While both MCML and CUDAMCML assumed perpendicular photon launch, this study modeled photon-skin interaction using Fresnel's equations to account for specular reflection. When photons

hit the skin at an angle, part of their energy is reflected due to the differing refractive indices, while the rest penetrates. To optimize for modern hardware, the number of blocks increased to 80, and threads per block were raised to 288.

3. Research Hypothesis and Testing Design

3.1. Research Hypothesis

Given Monte Carlo's powerful capability to simulate light interactions in complex multilayered media, in this study, we assume that the Monte Carlo Multilayer Media simulated data of diffuse reflectance of a specific type of human skin would approximately agree with the real data measured on a real human similar-skin type sample.

3.2. Testing Design

To verify the proposed hypothesis on the agreement between simulated and measured data, the fast MCML simulations (CUDAMCML) were conducted and measured data were collected for diffuse reflectance of the normal healthy skin condition at 03 different skin tones (Light, Moderate, Dark), at the wavelengths between 900 nm and 1700 nm. The general framework of our system is shown in Figure 3.

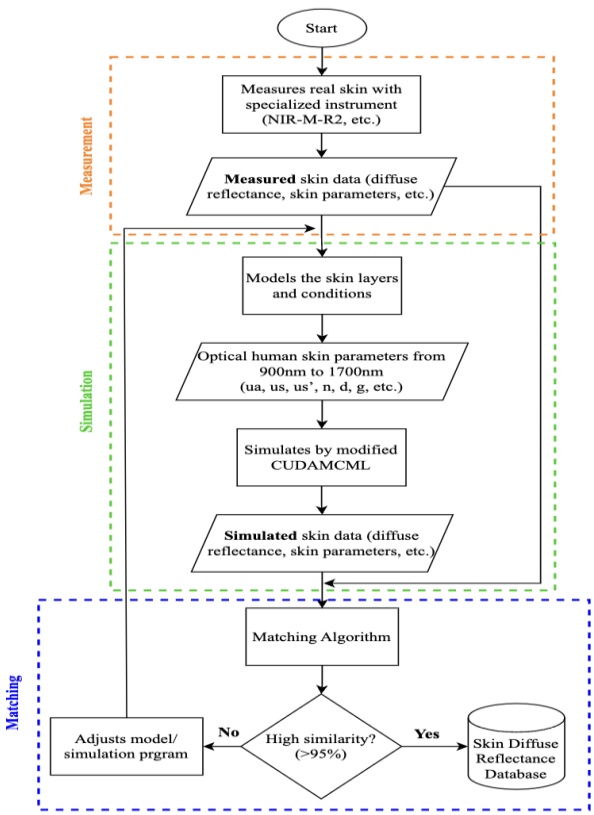

Figure 3. *The overall design of the system*

3.3. Testing Setup

For the collection of real data, measurements were taken from human skin samples representing light, moderate, and dark skin tones. Three samples with comparable skin conditions were gathered for each skin tone. The specific conditions of these samples, such as dryness or signs of aging, were carefully observed and recorded. This information was intended for later use in configuring the skin parameters for simulations. The measurement locations on the body were chosen randomly and included the inner forearms, the back of the hands, and the cheeks. Correspondingly, for the simulation data, skin parameters that mirrored these observed conditions were generated for each of the light, moderate, and dark skin tones.

3.4. Experimental setup

To gather diffuse reflectance data, the NIR-M-R2 scanning module was used, capturing readings in the 900 nm to 1700 nm range at 4 nm intervals, with wavelength accuracy of ±1nm [17]. Data was collected from 08 Vietnamese individuals across three skin tone categories (Light, Moderate, Dark) and three age groups (10-29, 30-49, 50-70 years). Measurements were taken from the inner forearms, backs of the hands, and cheeks. Figure 4 shows these measurement areas.

The NIR-M-R2 module uses angled lamps to illuminate the skin, collecting diffuse reflection through a slit while minimizing specular reflections. It calculates absorbance and diffuse reflectance based on the signal intensity. Measurements were conducted under standard indoor lighting, with the sapphire window gently pressed against the skin. Photographs were taken to document variations across the skin surface and ensure consistency. Multiple readings were taken per area, and the average was used as the representative value.

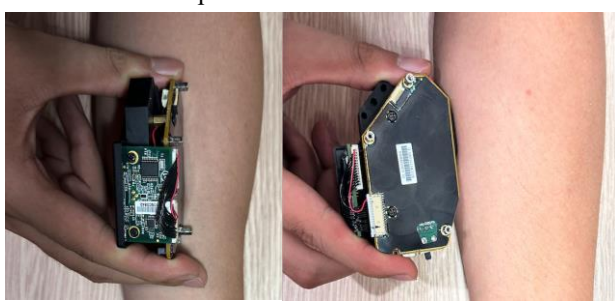

Figure 4. *A typical spectral imaging measurement on a forearm*

3.5. Simulation data collection setup

The described system is designed to simulate the interaction between light and skin, specifically to determine the diffuse reflectance, absorption, or transmittance of light. This simulation covers a wavelength range from 900 nm to 1700 nm, with increments of 4 nm. The simulation process itself consists of two main components: one dedicated to modeling the skin and another for executing the simulation. The skin modeling phase begins by defining the skin's parameters according to the values outlined in Table I.

For each simulation, an input file is utilized. This file specifies the optical properties for all four skin layers across various wavelengths, the total number of photons to be simulated, the configuration of the detection grid, and the angle at which the photon beam strikes the skin. A single simulation performed at one specific wavelength is referred to as a "run." The entire simulation for a particular skin model is considered complete once all designated wavelengths have been processed.

Table 1. *Descriptions, symbols, units, and ranges of parameter in the four layers*

Layer	Description	Symbol	General Value	Average Values
Stratum corneum	Volume fraction of water [12]	C_{wSC}	3-7%	5%
	The reduced scattering at 500nm [18]	$us'_{500nmSC}$	66.7cm^{-1}	66.7cm^{-1}
	The fraction of Rayleigh scattering [19]	$fRay_{SC}$	0.29	0.29
	The scattering factor [19]	$bMie_{SC}$	0.689	0.689
	Anisotropy factor [20]	g_{SC}	0.86-0.9	0,88
	Thickness [10]	d_{SC}	0.0009-0.004cm	0,00245cm
	Refractive index [21]	η_{SC}	1.5	1.5
Living epidermis	Volume fraction of melanin [11]	C_m	1.3-43%	22,15%
	Volume fraction of water [18]	C_{wLV}	10-20%	15%
	The reduced scattering at 500nm [18]	$us'_{500nmLV}$	66.7cm^{-1}	66.7cm^{-1}
	The fraction of Rayleigh scattering [19]	$fRay_{LV}$	0.29	0.29
	The scattering factor [19]	$bMie_{LV}$	0.689	0.689
	Anisotropy factor [20]	g_{LV}	0.8	0.8
	Thickness [13]	d_{LV}	0.0027-0.015cm	0,00885cm
	Refractive index [21]	η_{LV}	1.4	1.4
Dermis	Volume fraction of blood [22]	C_{blDER}	0.2-7%	3,60%
	Oxygen saturation [13]	S	50-95%	72,50%
	Volume fraction of water [13]	C_{wDER}	40-90%	65%
	The reduced scattering at 500nm [18]	$us'_{500nmDER}$	43.6cm^{-1}	43.6cm^{-1}
	The fraction of Rayleigh scattering [19]	$fRay_{DER}$	0.41	0.41
	The scattering factor [19]	$bMie_{DER}$	0.2-0.562	0,381
	Anisotropy factor [20]	g_{DER}	0.75	0.75
	Thickness [13]	d_{DER}	0.06-0.3cm	0,18cm
	Refractive index [21]	η_{DER}	1.37	1.37
Subcutis	Volume fraction of blood [23]	C_{blSUB}	5-20%	12,50%
	Oxygen saturation [23]	S	50-95%	72,50%
	Volume fraction of fat [23]	C_{fat}	40-70%	55%
	Volume fraction of water [23]	C_{wSUB}	40-90%	65%
	The reduced scattering at 500nm [18]	$us'_{500nmSUB}$	43.6cm^{-1}	43.6cm^{-1}
	The fraction of Rayleigh scattering [19]	$fRay_{SUB}$	0.41	0.41
	The scattering factor [19]	$bMie_{SUB}$	0.562	0.562
	Anisotropy factor [20]	g_{SUB}	0.75	0.75
	Thickness [13]	d_{SUB}	0.1-0.5cm	0,3cm
	Refractive index [21]	η_{SUB}	1.37	1.37

The CUDA Monte Carlo simulation generates diffuse reflectance data across various wavelengths for a given skin model. These models and their calculated reflectances are compared to existing data using a similarity score, guiding refinement of both the models and the simulation program. In addition to simulations, skin parameters can also be measured directly with specialized instruments, expanding the comprehensive database of human skin.

Skin models were developed by closely examining the measured areas to reflect the conditions of the study participants. The CUDAMCML simulation program was used to analyze the interaction between light and skin, examining how parameters and skin tones affect optical properties. The model developed in this study can be applied in any Monte Carlo-based simulation program, like CUDAMCML, by defining key parameters for each layer: thickness (d), anisotropy factor (g), refractive index (ηSC), absorption coefficient (μa), and scattering coefficient (μs).

Melanin content in the living epidermis determines skin color. To model this, we simulated three common skin tones encountered in Vietnamese people: lightly pigmented, moderately pigmented, and darkly pigmented. The melanin volume fraction was adjusted to 3-4% for lightly pigmented, 4-5% for moderately pigmented, and 6-7% for darkly pigmented samples. Other optical parameters were set for normal skin according to Table 1, which details values for normal skin.

4. Results and Evaluation

The captured images obtained from the measured skin samples are detailed in Table II. Given the high degree of similarity observed among the three samples collected for each distinct skin tone, the average diffuse reflectance data from samples of every skin tone category was selected for subsequent calculations and for comparison against the simulated data.

Table 2. *Captured images and diffuse reflectance results of the measured skin samples*

Skin tone	Light			Moderate			Dark		
Samples	Sample 1	Sample 2	Sample 3	Sample 1	Sample 2	Sample 3	Sample 1	Sample 2	Sample 3
Captured Images									

Figure 5 shows the average diffuse reflectance of the measured reflectances for lightly pigmented, moderately pigmented, and darkly pigmented individuals. The obtained diffuse reflectances were standardized.

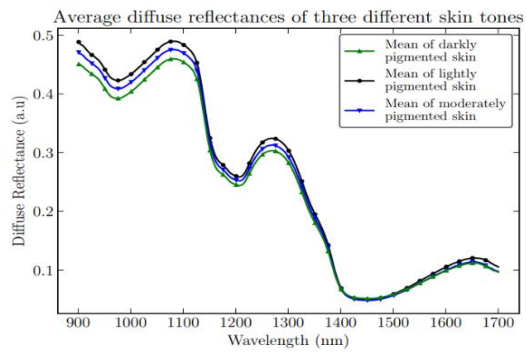

Figure 5. *Average diffuse reflectance of three different skin tones*

Results showed that people with light skin have the highest diffuse reflectances. Moderately pigmented people have lower skin reflectances, and the lowest reflectances are found in people with dark skin. The concentration of melanin directly correlates to the skin tone. People with darker skin have higher concentrations of melanin and can absorb more light compared to lighter skin individuals, and consequently have lower diffuse reflectance. The results thus agree with our assumptions.

To compare simulated and measured data, we calculated a similarity score (SS) using a modified Facebook Artificial Intelligence Similarity Search (FAISS) model [24]. For the 900-1700 nm wavelength range, the SS was derived from the mean Euclidean distance, $d(u, v)$, between the simulated (u) and real (v) reflectance values, as defined by the following equation [25]:

$$SS = \frac{1}{1+ d(u,v)} \quad (4.1)$$

It can be seen that for the considered skin tones, the simulated diffuse reflectances closely followed the measured reflectances. The similarities reached 96.45% for lightly pigmented skin, 96.4% for moderately pigmented skin, and 96.3% for darkly pigmented skin. This corresponds to an average discrepancy of only ~3.6%. There are high similarities between the measured and simulated reflectance for wavelengths between 900 and 1200 nm, and between 1400 and 1700 nm. The simulated diffuse reflectances at wavelengths from 1200 nm to 1360 nm suffer noticeable decreases compared to the measured reflectance. These drops are primarily caused by the difference in the water content of the measured and simulated samples. The water content of normal skin can vary greatly between each individual. These results agree with our assumptions about the effects of skin tones on the diffuse reflectances of the skin, and our method can accurately and correctly simulate the three skin tones: lightly pigmented, moderately pigmented, and darkly pigmented.

The comparisons between measured and simulated samples with different skin tones are illustrated in Figure 6.

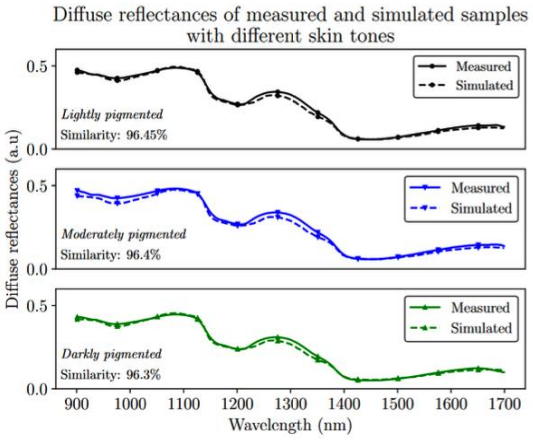

Figure 6. *Comparison between the diffuse reflectance of measured and simulated samples*

5. Conclusion

This research explored using Monte Carlo Multilayer Media Simulation to create a human skin database for diagnostic purposes. The hypothesis was validated by the alignment of simulation results with actual measurements. Unlike traditional, costly, and invasive methods, non-invasive spectroscopy techniques are favored for skin diagnosis, but their development is limited by the lack of comprehensive skin optical property databases. This study introduced an efficient skin modeling technique to rapidly expand the diffuse reflectance database.

A spectroscopy-based modeling approach was used, with four layers: stratum corneum, living epidermis, dermis, and subcutis, each defined by dominant components affecting optical properties. The study found that various skin conditions influenced these components. Simulations were run using the CUDAMCML program, which offered high speed and simplicity. Adjusting the refractive index of the stratum corneum to account for surface roughness was key.

Real-world data was collected using the NIR-M-R2 diffuse reflective module from InnoSpectra, measuring skin from 08 Vietnamese individuals across three areas: inner forearms, backs of hands, and cheeks. The data expanded the existing database and helped evaluate the modeling methodology. A similarity score showed that simulations of lightly pigmented skin, with varying dryness and aging, had over 96% similarity with measured results. Dry skin and older age increased diffuse reflectance, as did lighter skin tones. However, the skin on the cheeks showed unexpected behavior, likely due to the diversity in skin tones, conditions, and measurement variations.

Despite success, the method has limitations. CUDAMCML treats skin layers as flat structures and doesn't account for surface roughness or non-perpendicular light. It also lacks broader skin tone representation and conditions like melasma. Additionally, the measured database is small, with only 186 samples from 27 participants. Nevertheless, the methodology is effective for expanding the optical properties database, particularly for the inner forearms and backs of hands, where skin tone, dryness, and age can be accurately modeled.

6. Future works

The researchers plan to expand their work to include more skin areas and a broader range of skin tones from different regions. This expansion is vital for rapidly growing the database of human skin's optical properties, which is essential for developing AI-driven, non-invasive diagnostic tools for skin conditions. This enriched database will serve as the foundation for creating advanced, Machine Learning-based diagnostic tools to accurately identify various skin conditions through diffuse reflectance analysis.

Acknowledgement: This research was supported by the University of Danang's Funds for Science and Technology Development (project number B2023-DN02-20). We thank the LYDINC Institute of Education and Engineering - Technology and L.Y.D.I.N.C Co. Ltd., and the University of Danang – Danang International Institute of Technology (UD-DNIIT) for their technical support, equipment (especially the NIR scanner), and valuable contributions throughout the project.

REFERENCES

[1] H. W. Lim *et al.*, "The burden of skin disease in the United States", *Journal of American Academy of Dermatology*, vol. 76, no. 5, pp. 958-972.e2, 2017. https://doi.org/10.1016/j.jaad.2016.12.043

[2] D. Seth, K. Cheldize, D. Brown, and E. F. Freeman, "Global Burden of Skin Disease: Inequities and Innovations", *Current dermatology reports*, vol. 6, no. 3, pp. 204–210, 2017. https://doi.org/10.1007/s13671-017-0192-7

[3] N. Thanh, "Moi nam nguoi dan chi toi 75 ti USD de dieu tri benh ve da", *nld.com.vn,* Nov 21st , 2020. [Online]. Available: https://nld.com.vn/suc-khoe/moi-nam-nguoi-dan-chi-toi-75-ti-usd-de-dieu-tri-benh-ve-da-20201121161932819.htm [Accesed May 13, 2025].

[4] X. Mai, "Benh viem da tang manh trong nang nong", *tuoitre.vn,* Jun 14th, 2023. [Online]. Available: https://tuoitre.vn/benh-viem-da-tang-manh-trong-nang-nong-20230614001140849.htm [Accesed May 13, 2025].

[5] D. Yi, W. Yang, S. Z. Li, *Encyclopedia of Biometrics*, 2nd edition. MA: Springer, 2015.

[6] S. Jowett and T. Ryan, "Skin disease and handicap: An analysis of the impact of skin conditions", *Social Science & Medicine*, vol. 20, no. 4, pp. 425–429, 1985. https://doi.org/10.1016/0277-9536(85)90021-8

[7] L. C. Daniel, C. J. Heckman, J. D. Kloss, and S. L. Manne, "Comparing alternative methods of measuring skin color and damage", *Cancer Causes & Control*, vol. *20, no*. 3, pp. 313–321, 2008. https://doi.org/10.1007/s10552-008-9245-3

[8] G. Zonios, A. Dimou, I. Bassukas, D. Galaris, A. Tsolakidis, and E. Kaxiras, "Melanin absorption spectroscopy: new method for noninvasive skin investigation and melanoma detection", *Journal of Biomedical Optics*, vol. *13,* no. 1, pp. 14017, 2008. https://doi.org/10.1117/1.2844710

[9] M. Sasikala, S. Mohan, and S. Swarnakumari, "Highlights of Spectroscopic Analysis – A Review", *International Journal of Life Science and Pharma Research*, vol. 11, no. 2, pp. 136-145, 2021. https://doi.org/10.22376/ijpbs/lpr.2021.11.2.p136-145

[10] I. Chingovska, A. Anjos, and S. Marcel, *Encyclopedia of Biometrics,* 0th edition. Heidelberg: Springer, 2020.

[11] S. L. Jacques, "Optical absorption of melanin", *omlc.org*. [Online]. Available: https://omlc.org/spectra/melanin/[Accessed May 13, 2025].

[12] I. V. Meglinski and S. J. Matcher, "Quantitative assessment of skin layers absorption and skin reflectance spectra simulation in the visible and near-infrared spectral regions", *Physiological Measurement*, vol. 23, no. 4, pp. 741–753, 2002. https://doi.org/10.1088/0967-3334/23/4/312

[13] S. Li, M. Ardabilian, and A. Zine, "Quantitative Analysis of Skin using Diffuse Reflectance for Non-invasive Pigments Detection", in *Proc. 16th Int. Joint Conf. Comput. Vis. & Graph*, 2021, pp. 604-614.

[14] A. N. Bashkatov, E. A. Genina, and V. V. Tuchin, "Optical Properties of Skin, Subcutaneous, and Muscle Tissues: A Review", *Journal of Innovative Optical Health Sciences*, vol. 4, no. 1, pp. 9–38, 2011. https://doi.org/10.1142/s1793545811001319.

[15] G. V. G. Baranoski and A. Krishnaswamy, *Light & skin interactions: Simulations for Computer Graphics Applications*. Morgan Kaufmann, 2010.

[16] L. Wang, S. L. Jacques, and L. Zheng, "MCML - Monte Carlo modeling of light transport in multi-layered tissues", *Computer Methods and Programs in Biomedicine*, vol. 47, no. 2, pp. 131–146, 1995. https://doi.org/10.1016/0169-2607(95)01640-f.

[17] InnoSpectra Corporation, "NIR-M-R2", *inno-spectra.com*, 2021. [Online]. Available: https://www.inno-spectra.com/ueditor/php/upload/file/20220928/1664336948607909.pdf [Accesed May 13, 2025].

[18] S. L. Jacques, "Optical properties of biological tissues: a review", *Physics in Medicine and Biology*, vol. 58, no. 11, pp. R37–R61, 2013. https://doi.org/10.1088/0031-9155/58/11/r37

[19] E. Salomatina, B. Jiang, J. Novak, and A. N. Yaroslavsky, "Optical properties of normal and cancerous human skin in the visible and near-infrared spectral range", *Journal of Biomedical Optics*, vol. 11, no. 6, pp. 064026, 2006. https://doi.org/10.1117/1.2398928

[20] S. V. Patwardhan, A. P. Dhawan, and P. A. Relue, "Monte Carlo Simulation of Light-Tissue Interaction: Three-Dimensional Simulation for Trans-Illumination-Based Imaging of Skin Lesions", *IEEE Trans. Biomed. Eng.*, vol. 52, no. 7, pp. 1227-1236, 2005. https://doi.org/10.1109/TBME.2005.847546

[21] K. Martin, *The Internet Journal of Vibrational Spectroscopy*, 2nd edition. UK: Ventacon, 1999.

[22] A. J. Rodriguez, *et al.* "Skin optical properties in the obese and their relation to body mass index: a review". *Journal of Biomedical Optics*, vol. 27, no. 3, pp. 030902, 2022. https://doi.org/10.1117/1.jbo.27.3.030902

[23] G. Nishimura, I. Kida, and M. Tamura, "Characterization of optical parameters with a human forearm at the region from 1.15 to 1.52 microm using diffuse reflectance measurements", *Phys. Med. Biol.*, vol. 51, no. 12, pp. 2997-3011, 2006. https://doi.org/10.1088/0031-9155/51/11/021

[24] H. Jégou, *et al.* "faiss", *github.com*. [Online]. Available: https://github.com/facebookresearch/faiss/wiki/Faiss-indexes [Accesed May 13, 2025].

[25] M. Greenacre, *International Encyclopedia of Education,* 3rd edition. Elsevier, 2010.